ANTIOXIDANTS & REDOX SIGNALING
Volume 9, Number 4, 2007

DOI: 10.1089/ars.2006.1392

Original Research Communication

Integrin-Mediated Cell Adhesion and Spreading Engage Different Sources of Reactive Oxygen Species

MARIA LETIZIA TADDEI,[1] MATTEO PARRI,[1] TOMMASO MELLO,[2] ALFONSO CATALANO,[3] ALAN D. LEVINE,[4] GIOVANNI RAUGEI,[1,5] GIAMPIETRO RAMPONI,[1,5] and PAOLA CHIARUGI[1,5]

ABSTRACT

The tightly regulated production of intracellular reactive oxygen species (ROS) participates in several biologic processes such as cellular growth, programmed cell death, senescence, and adhesion. It is increasingly evident that the same enzymatic processes that were originally linked to ROS generation during host defence or apoptosis execution are also involved in redox-mediated signal transduction. We investigated in murine NIH3T3 fibroblasts the contribution of a variety of redox-dependent events during signal transduction initiated by integrin engagement due to fibronectin stimulation and report that a mitochondrial ROS release occurs, strictly confined to the early phase of extracellular matrix (ECM) contact (10 min). Besides, 5-lipoxygenase (5-LOX) is engaged by integrin receptor ligation as another ROS source, contributing to the more-intense, second ROS burst (45 min), possibly orchestrating the spreading of cells in response to ECM contact. To define a potential mechanism for ROS signaling, we demonstrate that on integrin recruitment, the Src homology-2 domain–containing phosphatase 2 (SHP-2) undergoes a reversible oxidization/inactivation to which mitochondrial and 5-lipoxygenase ROS contribute differentially. In keeping with a key role of oxidants during integrin signaling, the inactivation of SHP-2 prevents the dephosphorylation and inactivation of SHP-2 substrates (p125FAK and SHPS-1), thus enabling the continued propagation of the signal arising by integrin engagement. *Antioxid. Redox Signal.* 9, 469–481.

INTRODUCTION

It is currently recognized that reactive oxygen species (ROS) are not only a toxic by-product of aerobic metabolism but, when produced at lower and regulated levels, can act as second messengers involved in the transduction of mitogenic, differentiation, and adhesion signals (18–20). The production of ROS on neutrophil activation involves both NADPH oxidase and myeloperoxidase generation of superoxide anions in a phenomenon called the "oxidative burst" (38). In nonphagocytic cells, cytosolic oxidases produce ROS at the plasma membrane during stimulation with epidermal growth factor (1), platelet-derived growth factor (44), angiotensin-II (23), thrombin (16), lysophosphatidic acid (9, 16), interleukin-1, tumor necrosis factor-α (51), and transforming growth factor-β1 (3). During the transduction of these signaling events, inhibition of protein-tyrosine phosphatases (PTP) potentiates tyrosine kinase phosphorylation, thus promoting the propagation of the mitogenic stimulus (1, 29). During tumor necrosis factor-α stimulation, Rac1-dependent ROS production is blocked by inhibition of 5-lipoxygenase (5-LOX), suggesting that ROS generation is de-

[1]Department of Biochemical Sciences, University of Florence, Florence, Italy.
[2]Farmacogenomic Foundation FiorGen, Polo Scientifico,Florence, Italy.
[3]Department of Molecular Pathology and Innovative Therapies, Polytechnic University of Marche, Ancona, Italy.
[4]Departments of Medicine, Pathology, and Pharmacology, Case Western Reserve University School of Medicine, Cleveland, Ohio.
[5]Center for Research, Transfer and High Education Study at Molecular and Clinical Level of Chronic, Inflammatory, Degenerative and Neoplastic Disorders for the Development on Novel Therapies, Florence, Italy.

pendent on synthesis of arachidonic acid and its subsequent metabolism to leukotrienes by 5-LOX (49). Furthermore, Peppelenbosch *et al*. (3, 36) demonstrated that Rac is essential for EGF-induced arachidonic acid production and subsequent generation of leukotrienes, and Chiarugi *et al*. (14) recently suggested that 5-LOX is the main source of ROS during integrin-mediated cell adhesion. A further source of intracellular ROS is the mitochondria compartment where oxygen is converted to $O_2^{\bullet -}$ by ubiquinone-mediated one-electron reduction (5). Mitochondrial ROS production was originally associated only with apoptosis execution (6), but more recently it has been linked to tumor necrosis factor-α (41), hypoxia (8), and integrin signaling (48).

Several lines of evidence demonstrate that these intracellularly produced ROS are specific second messengers able to affect protein phosphorylation by the reversible modification of cytosolic targets (1, 44). The key targets of ROS action are cysteine residues that can be oxidized to cysteine sulfenic acid or disulfide and then readily reduced to cysteine by various cellular reductants. Several molecules identified as vulnerable to oxidation by hydrogen peroxide include the nuclear factor κB (43), activator protein-1 (33), hypoxia-inducible factor (47), p53 (37), and several members of the PTP family (31). Several reports have delineated that PTPs are the targets of reversible oxidation by ROS produced during both mitogenic and integrin signaling (11, 13). In particular, PTP1B is oxidized during EGF stimulation in A431 cells (1), Src homology domain phosphatase-2 is transiently oxidized in response to platelet-derived growth factor and T-cell–receptor activation (28, 31), and low-molecular-weight PTP (LMW-PTP) is reversibly oxidized during both PDGF and integrin signaling (12, 14). The oxidation of PTPs is due to the presence of an invariant Cys residue in the signature motif of the active-site cleft of the PTPs members. Such modification results in inhibition of activity because the oxidized Cys can no longer function as a phosphate acceptor during the first step of the PTP-catalyzed reaction. It is generally thought that the production of ROS during stimulation with growth factors and the consequent inactivation of PTP may contribute to enhanced or extended tyrosine phosphorylation–dependent signaling, thereby promoting a burst of protein tyrosine kinase activity (50).

In this report, we dissect the specific contribution of different ROS metabolic events to early and late cell adhesion. We identify SHP-2 as a target of ROS production during integrin recruitment and propose that its reversible oxidation/inhibition enhances the propagation of integrin signaling.

MATERIALS AND METHODS

Materials

Unless specified, all reagents were obtained from Sigma (St. Louis, MO). NIH3T3 mouse fibroblasts were purchased from ATCC (ATCC). γ-[^{32}P]ATP, Sepharose G-50 column, protein A Sepharose, and Enhanced Chemi-Luminescence kit were from Amersham Pharmacia Biotech (Milan, Italy); PVDF membrane was from Millipore (Bedford, MA); anti-SHP-2 and anti-FAK antibodies were from Santa Cruz Biotechnology (Santa Cruz, CA); and anti-SIRPα1/SHPS-1 and anti-phosphotyrosine, clone 4G10, were from Upstate Biotechnology, Inc. (Charlottesville, VA). TRITC-phalloidin, DCF-DA, tetramethylrhodamine, ethyl ester, perchlorate (TMRE), and *N*-(biotinoyl)-*N*′-(iodoacetyl)-ethylenediamine (BIAM) were obtained from Molecular Probes (Milan, Italy); avidin-HRP conjugate was from BIO-RAD (Carlsbad, CA); BCA protein assay reagent was from Pierce (Rockford, IL). wtSHP-2 and dnSHP-2 cDNA in PJ3omega were gifts from Dr. M. Lackmann (Monash University, Australia); and pBABE-GFP-RacN17 and RacV12 were gifts from Dr. C. Deroanne (Nice, France). 2-(12-Hydroxydodeca-5,10-diynyl)-3,5,6-trimethyl-1,4-benzoquinone (AA-861) was from Biomol Int (U.S.A.)

Cell culture and transfection

NIH3T3 were routinely cultured in DMEM supplemented with 10% fetal calf serum (FCS) in 5% CO_2 humidified atmosphere. For transient transfections, pBABE-GFP-RacN17, pBABE-GFP-RacV12, wtSHP-2PJ3omega, and dnSHP-2PJ3omega plasmids were purified by using QIAfilter Plasmid Midi kit (Qiagen, Italy) and transfected by using Lipofectamine 2000 (Invitrogen, CA) according to the manufacturer's instructions. The efficiency of transient transfections was measured by flow-cytometry analysis with a BD-LSR cytofluorimeter.

Cell adhesion

In total, 10^6 cells were serum starved for 24 h before detaching with 0.25% trypsin for 1 min. Trypsin was blocked with 0.2 mg/ml soybean trypsin inhibitor, and cells were resuspended in 3 ml/10-cm dishes of fresh medium, maintained in suspension for 30 min at 37°C, and then directly seeded onto precoated dishes treated overnight with 10 μg/ml human fibronectin. Control cells were kept in suspension and then plated onto dishes pretreated with 10 μg/ml polylysine.

Determination of intracellular H_2O_2 in in vivo assay

The 3×10^5 NIH3T3 cells were kept for 30 min at 37°C in suspension and then directly seeded onto fibronectin precoated glass-bottom dishes for confocal analysis. Then 5 μg/ml DCF-DA was added, and ROS production observed during the following 45 min by using a laser scanning confocal microscope (model LEICA TCS SP2 with Acusto-Optic Beam Splitter DMIRE2) equipped with an Ar laser and two He/Ne lasers (543 and 633 nm). Time-lapse image acquisition was performed by using Leica LCS software, whereas subsequent image processing was done with Unlead Video Studio software, version 7. To ensure complete signal separation, DCF-DA and TMRE channels were recorded by sequential (between-lines) scanning. For experiments performed in the presence of rotenone to block mitochondrial release of ROS, cells were treated as previously described, except for the presence of 5 μ*M* rotenone from the beginning of suspension. For mitochondrial labeling, 250 n*M* TMRE was added 10 min before seeding the cells.

In vitro assay

Intracellular production of H_2O_2 was assayed as described previously (35). Three min before the end of adhesion or suspension, cells were treated with 5 μg/ml DCF-DA. After PBS washing, cells were lysed in 1 ml of RIPA buffer (50 m*M* Tris-HCl, pH 7.5, 150 m*M* NaCl, 1% Triton X-100, 2 m*M* EGTA, 1 m*M* sodium orthovanadate, 1 m*M* phenyl-methanesulphonyl fluoride, 10 μg/ml aprotinin, 10 μg/ml leupeptin), and analyzed immediately with a fluorescent spectrophotometer at 510 nm. Data were normalized to total protein content.

NBT staining

NIH3T3 cells were kept in suspension and then plated onto polylysine- or fibronectin-coated dishes in DMEM without phenol red. Then 0.5 mg/ml of NBT was added for 30 min. To quantify NBT precipitation, cells were washed twice with 70% methanol and fixed for 5 min in 100% methanol. After the wells were allowed to air dry, the formazan was solubilized with 120 μl 2 *M* KOH and 140 μl DMSO. The OD was read in a plate reader at 590 nm (40).Values were normalized to total protein content.

Immunoprecipitation and Western blot analysis

Cells were lysed for 20 min on ice in 1 ml of complete RIPA lysis buffer (50 m*M* Tris-HCl, pH 7.5, 150 m*M* NaCl, Triton X-100, 2 m*M* EGTA, 1 m*M* sodium orthovanadate, 1 m*M* phenyl-methanesulphonyl fluoride, 10 μg/ml aprotinin, 10 μg/ml leupeptin). Lysates were clarified by centrifugation and immunoprecipitated for 4 h at 4°C with 2 μg of the specific antibodies. Immunocomplexes were collected on protein A-Sepharose, separated by SDS-polyacrylamide gel electrophoresis, and transferred onto PVDF membrane. Immunoblots were probed first with specific antibodies in 1% bovine serum albumin, 0.05% Tween 20 in TBS buffer (10 m*M* Tris, pH 7.5, 100 m*M* NaCl), and then with secondary antibodies conjugated with horseradish peroxidase, washed, and developed with the enhanced chemiluminescence kit. Quantity-One software (Bio-Rad Laboratories) was used to perform quantitative analyses.

In-gel phosphatase assay

For detection of PTP activity, we prepared a 10% SDS-polyacrylamide gel containing 10^5 cpm/ml of [^{32}P]-labeled substrate as described previously (4). In brief, 0.3 mg of substrate [poly-(glutamate:tyrosine)] was dissolved in kinase buffer (150 m*M* NaCl, 2 m*M* $MgCl_2$, 12 m*M* Mg acetate, 0.02% Triton, 5% glycerol, 50 m*M* Hepes pH 7.4, 0.1 *M* ATP) and incubated with 200 μCu of γ-[^{32}P]ATP, 2.5 U EGF receptor, and 500 ng EGF for 18 h at 37°C. The substrate was then precipitated by adding an equal volume of 20% trichloroacetic acid. After centrifugation at 12,000 *g* for 10 min, the pellet was resuspended in 100 μl of 2 *M* Tris, pH 7.2, and purified via a Sepharose G-50 column equilibrated with 50 m*M* imidazole, pH 7.2. Cells were lysed in 25 m*M* sodium acetate, 1% Nonidet P-40, 150 m*M* NaCl, 10% glycerol, 100 μg/ml catalase, and protease inhibitor cocktail, as described earlier. In the modified version of the technique, used to detect oxidized PTPs, 10 m*M* iodoacetic acid was added to the samples, after degassing the buffer (31). Then 15 μg of total protein was loaded onto the radiolabeled gel. After electrophoresis, gels were sequentially washed for the indicated times at room temperature in ~200 ml of the following buffers: buffer 1 (overnight): 50 m*M* Tris, pH 8, and 20% isopropanol; buffer 2 (twice, for 30 min): 50 m*M* Tris, pH 8, and 0.3% β-mercaptoethanol; buffer 3 (90 min): 50 m*M* Tris, pH 8, 0.3% β-mercaptoethanol, 6 *M* guanidine hydrochloride, and 1 m*M* EDTA; buffer 4 (three washes for 1 h each): 50 m*M* Tris, pH 7.4, 0.3% β-mercaptoethanol, 1 m*M* EDTA, and 0.04% Tween 20; buffer 5 (overnight): 50 m*M* Tris, pH 7.4, 0.3% β-mercaptoethanol, 1 m*M* EDTA, 0.04% Tween 20, and 4 m*M* DTT. Gels were then stained with Coomassie brilliant blue, destained in 40% methanol and 10% acetic acid, dried, and analyzed by using a Cyclone system (Perkin Elmer).

Immunohistochemistry

Presuspended NIH3T3 was seeded onto coverslips, washed with PBS, and fixed in 3% paraformaldehyde for 20 min at 4°C. Fixed cells were permeabilized with three washes with TBST (50 m*M* Tris/HCl, pH 7.4, 150 m*M* NaCl, 0.1% Triton X-100) and then blocked with 5.5% horse serum in TBST for 1 h at room temperature. Cells were incubated for 1 h with 50 μg/ml phalloidin-TRITC in TBS (50 m*M* Tris/HCl, pH 7.4, 150 m*M* NaCl). After extensive washes in TBST, cells were mounted with glycerol plastine and observed under a laser scanning confocal microscope (model LEICA TCS SP2 with Acusto-Optic Beam Splitter) equipped with a five-line Ar laser and two He/Ne lasers (lines 543 and 633).

Statistical analysis

All experiments were done at least in triplicate. Data are expressed as mean ± standard deviation. Statistical analysis of the data was performed by Student's *t* test; p values ≤ 0.05 were considered statistically significant.

RESULTS

ROS production during cell adhesion

Cell adhesion onto extracellular matrix (ECM) is a physiologic event reported to be linked to considerable production of intracellular ROS. Therefore, we followed the kinetics of ROS production during integrin-mediated cell adhesion with two different redox-sensitive probes: 2′,7′-dichlorofluorescein diacetate (DCF-DA), selectively responsive to hydrogen peroxide, and nitroblue tetrazolium (NBT), which is sensitive to superoxide (21) (Fig. 1A and B). Both superoxide and hydrogen peroxide generation have similar kinetics, as they increase after 10 min of adhesion, reach a peak at 45 min, and then decrease back to basal level within 2 h. Recently we demonstrated that integrin-induced cell spreading correlates with a 5-LOX–dependent oxidant increase and that these ROS play a key role as integrin signaling messengers (14). In addition, the involvement of a mitochondrial metabolism during integrin-receptor engagement has been linked to a Rac-dependent increase in intracellular ROS (48). To investigate

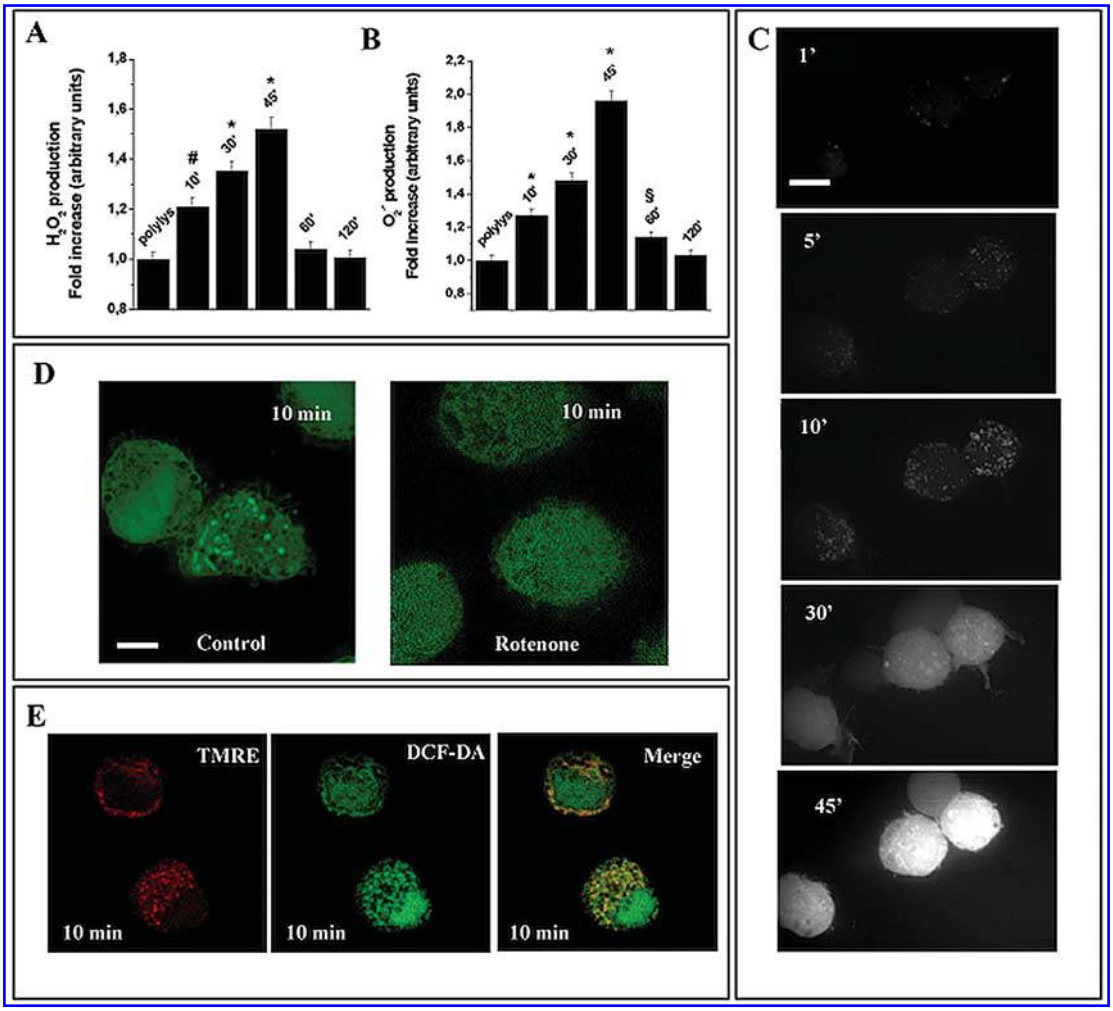

FIG. 1. ***In vivo*** **ROS production during cell adhesion.** (**A**) 10^6 cells were serum starved for 24 h before detaching and maintaining in suspension with gentle agitation for 30 min at 37°C. Cells were then seeded onto polylysine- or fibronectin-coated dishes for the indicated times. The 5 μ*M* DCF-DA was added 3 min before the end of each incubation period. After lysis, a fluorimetric analysis was performed. Values were normalized on the basis of protein content. #$p < 0.005$ vs. polylys; *$p < 0.001$ vs. polylys. (**B**) Cells were treated as in **A**, except that 5 mg/ml NBT was added for 30 min before the end of each incubation period. Reduced NBT was quantified as described in Materials and Methods. Values were normalized on the basis of protein content. One of three experiments is shown. §$p < 0.01$ vs. polylys; *$p < 0.001$ vs. polylys. (**C**) An NIH3T3 cell suspension was plated onto glass confocal dishes precoated with fibronectin. The 5 μg/ml DCF-DA was added, and the kinetics of ROS production was observed in real time under a laser scanning confocal microscope (model Leica TCS SP2 with Acusto-Optic beam Splitter). Single images show 1, 5, 10, 30, and 45 min of adhesion. Bar, 10 μm. (**D**) A similar experiment was performed in the absence or presence of 5 μ*M* rotenone added at the initiation of suspension. Bar, 5 μm. (**E**) An adhesion experiment was performed as in **C**, except for the presence of 250 n*M* TMRE. The superimposition of the DCF-DA signal (green fluorescence) and TMRE signal (red fluorescence) is indicated by yellow fluorescence. The results are representative of three independent experiments. Bar, 10 μm**.**

the contribution of both ROS sources during cell adhesion and spreading onto ECM ligands, we evaluated by real-time confocal microscopy ROS production using the DCF-DA probe (Fig. 1C). During the early phase of cell adhesion (within 10 min), ROS are produced in multiple, closed, and defined compartments. In contrast, thereafter, oxidant production becomes more diffuse in the cytosol at greatly enhanced concentrations. The involvement of a mitochondrial source during integrin-receptor engagement has been further linked to a Rac-dependent increase in intracellular ROS (48). To test the possibility that the compartments for the early production of ROS may be mitochondria, we used rotenone (rot), a selective inhibitor of mitochondrial superoxide production. As shown in Fig. 1D, incubation of fibroblasts with rotenone during cell adhesion completely prevents the formation of ROS within these intracellular compartments, whereas cytoplasmic oxidant production is only marginally affected (not shown). Furthermore, double-labeling confocal analysis was carried out during cell spreading, by using the redox-sensitive probe DCF-DA and the mitochondrial tracker tetramethylrhodamine ethyl ester, perchlorate (TMRE). Superimposition of the two images suggests that during the early contact between cells and ECM, mitochondria are involved in ROS production (Fig. 1E).

Recently we demonstrated that integrin-induced cell spreading is correlated with a 5-LOX–dependent oxidant increase and that these ROS play a key role as integrin-signaling messengers (14). To characterize the cellular locales involved in ROS production during the early and late phases of cell adhesion, we analyzed the effect of selective inhibitors of both mitochondrial- and 5-LOX–derived ROS within adhering NIH3T3 cells. For this purpose, we used nordihydroguaiaretic acid (NDGA) and 2-(12-hydroxydodeca-5,10-diynyl)-3,5,6-trimethyl-1,4-benzoquinone (AA-861) to block 5-LOX, and rotenone and antimycin A to inhibit mitochondrial ROS release. Based on the main effectiveness of these inhibitors at 10 or 45 min after adhesion (Fig. 2A), we conclude that mitochondria contribute mainly to the early phase of ROS generation, whereas 5-LOX is responsible for both phases of integrin-mediated oxidant production, although it contributes more strongly to the late phase of signaling.

Several lines of evidence underscore the involvement of the small GTPase Rac-1 in ROS production by either 5-LOX or NADPH oxidase pathways during both growth factor and integrin stimulation (27, 49). Furthermore, Werner *et al*. (48) suggest that the mitochondrial pathway involved in ROS production during the engagement of integrin receptors is mainly Rac dependent. To investigate the involvement of the small GTPase Rac during early and late adhesion, we analyzed the production of ROS in NIH3T3 transiently overexpressing the constitutively active and the dominant negative Rac1 mutants, RacV12 and RacN17, respectively. The percentage of cells expressing RacV12 and RacN17 was 58.4% and 44%, respectively, as evaluated by flow cytometry analysis. Our results demonstrate that Rac1 is involved mainly in the late burst of ROS, although a minor Rac dependency occurs in early, mitochondrial-mediated oxidant synthesis (Fig 2B). These findings enforce the idea that, at least in our cellular model, Rac is involved in both mitochondrial and 5-LOX–dependent ROS production.

Taken together, these results indicate that on integrin stimulation, two different phases are apparent: an early step characterized mainly by a release of ROS from both mitochondria and 5-LOX, and a later phase in which ROS production is mainly cytoplasmic and driven exclusively by 5-LOX.

Mitochondrial and cytoplasmic ROS differently contribute to cell adhesion

To investigate the role of mitochondrial and cytoplasmic ROS during integrin-mediated cell adhesion and spreading, we selectively inhibited the activity of each ROS pathway throughout both the early and late phases of adhesion. Figure 3A shows that cell spreading is affected mainly by NDGA and AA-861, because in the presence of these 5-LOX inhibitors, cells remain round and are not completely spread. In contrast, in cells treated with rotenone and antimycin A, the cell body appears to be less elongated, suggesting a defective cytoskeletal organization. Analysis of cytoskeleton architecture by phalloidin staining for actin fibers confirms that NDGA and AA-861 treatment completely impairs the overall cytoskeleton organization, whereas rotenone and antimycin A administration leads to incomplete and delayed spreading, characterized by defects in F-actin stress fiber formation (Fig. 3B). Furthermore, the contribution of the mitochondrial

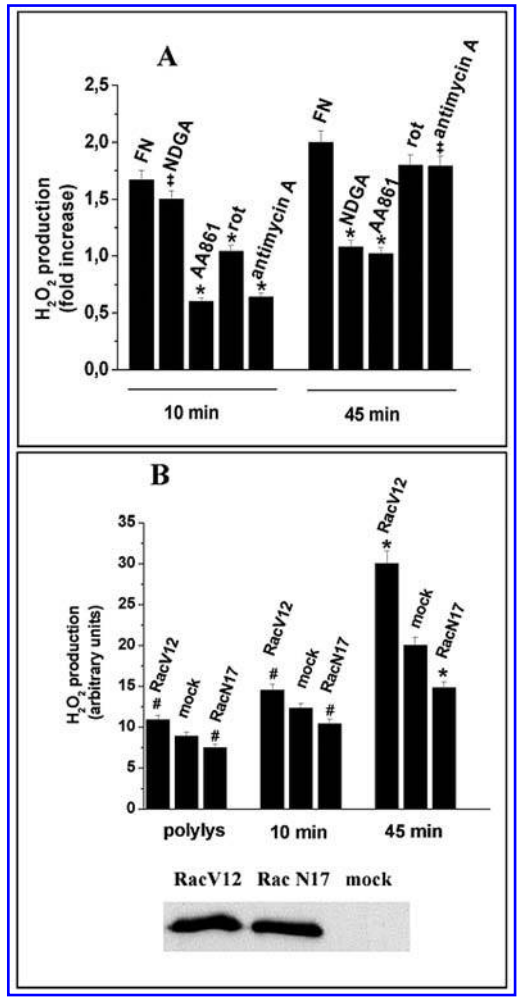

FIG. 2. Mitochondrial and cytoplasmic ROS are produced during different phases of cell adhesion. (**A**) Cells were serum starved for 24 h before detaching and maintaining in suspension with gentle agitation at 37°C for 30 min. The 3 x 10^4 cells were plated into individual wells of a polylysine- or fibronectin-coated 96-multiwell plate for the indicated times. The 10 μ*M* NDGA, 15 μ*M* AA-861, 1 μ*M* antimycin A, or 5 μ*M* rotenone was added for 20 min during the early and late phases of adhesion: for early adhesion, inhibitors were added 10 min before the end of suspension; for late adhesion, inhibitors were added 10 min after adhesion. Hydrogen peroxide production was evaluated with DCF-DA as described in Materials and Methods. Values were normalized on the basis of protein content. The bar graphs represent the ratio between the ROS content of fibronectin- and polylysine-seeded cells. Values are expressed as mean ± SD of triplicate samples. *$p < 0.001$ vs. FN at the same time; ‡$p \leq 0.05$ vs. FN at the same time. (**B**) NIH3T3 cells were transiently transfected with pEGFP-RacV12, pEGFP-RacN17, and pEGFP alone. At 24 h after transfection, cells were serum starved for 24 h before detaching and maintaining in suspension for 30 min at 37°C. Cells were then plated onto polylysine- or fibronectin-coated dishes for 10 or 45 min. Hydrogen peroxide production was evaluated with DCF-DA, as described in Materials and Methods. Values were normalized on the basis of protein content. The efficiency of transfection was evaluated by anti-Rac Western blot and flow-cytometry analysis. Values are expressed as mean ± SD of quadruplicate samples. *$p < 0.001$ vs. mock at the same time; #$p < 0.005$ vs. mock at the same time or vs. mock on polylys.

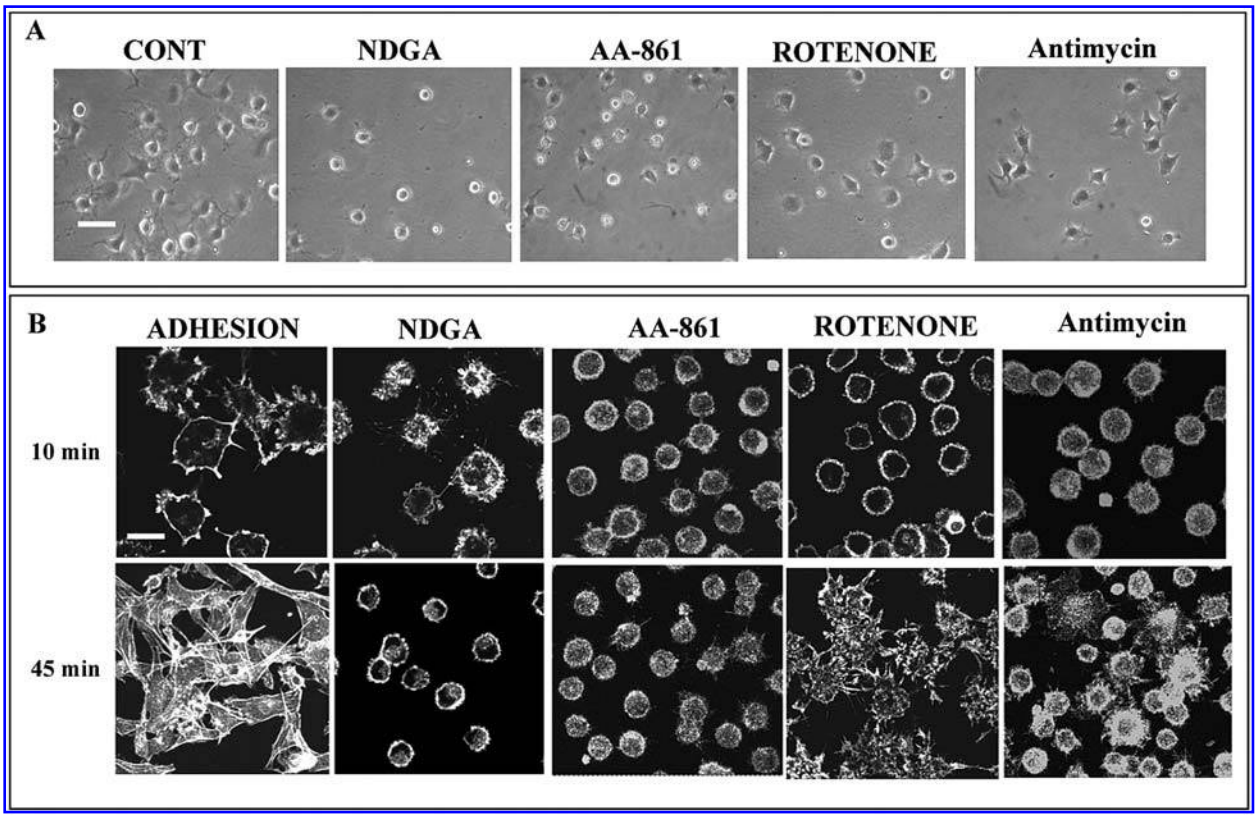

FIG. 3. Differential role of mitochondrial and cytoplasmic ROS during early and late adhesion. (**A**) 10^5 cells were serum starved for 24 h, detached, and kept in suspension at 37°C for 30 min. The 10 μ*M* NDGA, 15 μ*M* AA-861, 1 μ*M* antimycin A, or 5 μ*M* rotenone was added 10 min before seeding the cells onto fibronectin-coated dishes. Photographs of cells were taken with a phase-contrast microscope (Nikon) 2 h after adhesion. Bar, 40 μm. (**B**) Cells were treated as in **A**, except that 10 μ*M* NDGA, 15 μ*M* AA-861, 1 μ*M* antimycin A, or 5 μ*M* rotenone was added for 20 min during the early and late phases of adhesion: for early adhesion, inhibitors were added 10 min before the end of suspension; for late adhesion, inhibitors were added 10 min after adhesion. Cells were fixed, labeled with TRITC-phalloidin, and observed under a laser scanning confocal microscope. Bar, 20 μm.

and 5-LOX oxidant pathways appears to affect different phases of integrin-mediated cell adhesion. In particular, NDGA and AA-861 inhibit both early adhesion and late cell spreading, suggesting a role of 5-LOX–derived ROS in both the early contact of cells with ECM and in orchestrating the cytoskeleton organization during spreading of cells in response to ECM contact. Conversely, rotenone and antimycin A appear to affect mainly the early adhesion in response to ECM ligands, indicating mitochondrial ROS as mediators of the initial steps of cell contact with ECM. Taken together, these results indicate that on integrin stimulation, two different phases are apparent: an early step, mainly driving focal adhesion contacts, correlates with mitochondrial release of ROS. Later on, a following phase is concurrent with cell spreading and the organization of actin stress fibers, in which ROS production is mainly cytoplasmic.

SHP-2 is a target of adhesion-dependent ROS production

Previous reports demonstrated that intracellular ROS generated on integrin engagement are essential molecules acting as signal-transducing messengers (14). Protein tyrosine phosphatases (PTPs) are redox-sensitive proteins due to the presence of the active site cysteine and are among the possible targets of ROS originated in response to integrin engagement. The reversible oxidation and hence inactivation of PTP family members was demonstrated for PTP1B (29), LMW-PTP (12), and SHP-2 in response to growth factor stimulation (31) and T cell–receptor activation (28). Recently, LMW-PTP has been indicated as a target for redox signaling after integrin engagement (14). To explore the possible involvement of other PTPs in redox signaling during cell adhesion, we analyzed the redox state of other intracellular PTPs. To this purpose, we performed a modified PTP in-gel assay in which the active site cysteine of the *in vivo* reduced PTPs is irreversibly alkylated with iodoacetic acid, whereas oxidized PTPs are not alkylated. In the assay, the cell lysate was subjected to modified SDS-PAGE, in which a radioactively labeled PTP substrate was cast and the proteins in the gel were renatured in the presence of reducing agent. Under these conditions, only the activity of those PTPs that were oxidized on integrin engagement was recovered and visualized by the appearance of a clear, white area of dephosphorylation in the gel. A kinetic analysis of PTP redox regulation during cell adhesion shows that after 10 min of adhesion, many PTPs were oxidized (Fig. 4A). The oxida-

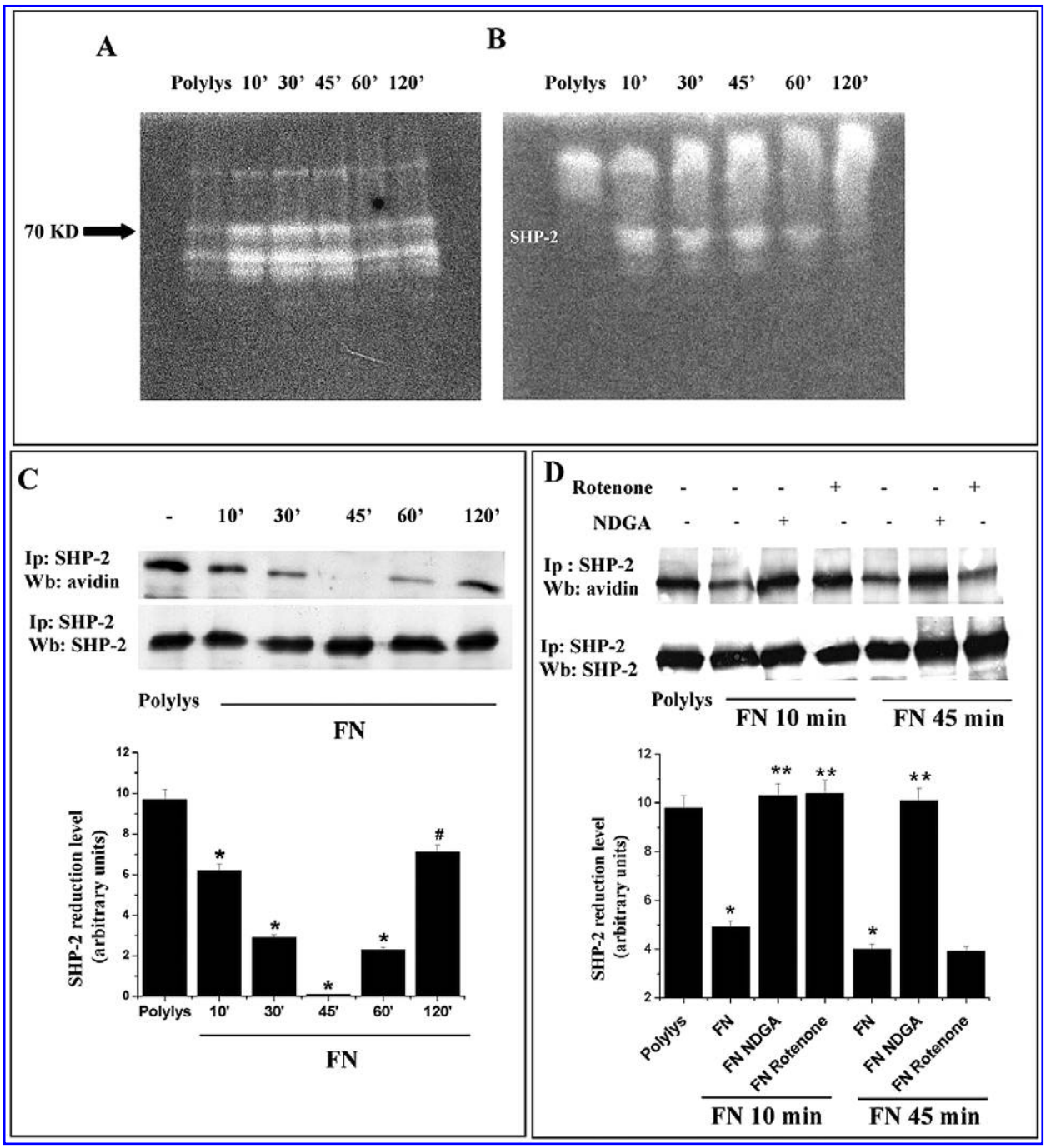

FIG. 4. SHP-2 is oxidized and inactivated during cell adhesion. (**A**) NIH3T3 cells were serum starved for 24 h before detaching and maintaining in suspension with gentle agitation for 30 min at 37°C. Cells were then seeded onto polylysine- or fibronectin-coated dishes for the indicated times. Lysates were prepared in the presence of 10 m*M* IAA and subjected to in-gel PTP assay. The results shown are representative of three independent experiments. (**B**) Cells were treated as in **A**, except that SHP-2 was immunoprecipitated from total cell lysate and then subjected to in-gel PTP assay. One of three experiments is shown. (**C**) Cells were treated as in **A**, except that they were lysed in RIPA buffer plus 40 μ*M* BIAM. SHP-2 was immunoprecipitated from total cell lysates. Samples were divided in half: an HRP-avidin and an anti-SHP-2 immunoblot were performed. A bar graph obtained from densitometry analysis of triplicate experiments normalized relative to loading controls is shown. *$p < 0.001$ vs. polylys; #$p < 0.005$ vs. polylys. (**D**) Cells were treated as in **A**, except that 10 μ*M* NDGA or 5 μ*M* rotenone was incubated for 20 min during the early and late phases of adhesion: for early adhesion, inhibitors were added 10 min before the end of suspension; for late adhesion, inhibitors were added 10 min after adhesion. Cells were lysed in RIPA buffer plus 40 μ*M* BIAM. SHP-2 was immunoprecipitated from total cell lysates, and an avidin-HRP immunoblot was performed. The blot was stripped and reprobed with anti-SHP-2 antibodies. A bar graph obtained from densitometry analysis of triplicate experiments normalized to loading controls is shown. *$p < 0.001$ vs. polylys; **$p < 0.001$ vs. FN at the same time.

tion/inactivation reaches a peak within 45 min of adhesion and then returns to the resting level almost completely within 1 h. We focused our attention on a PTP of ~70 kDa that is strongly oxidized during cell adhesion and may be a candidate in the regulation of cell spreading. Because the Src homology-2 domain–containing phosphatase (SHP-2) is required for integrin-evoked cell spreading, migration, and extracellular signal-regulated kinase (ERK) activation (52), we speculated that this 70-kDa PTP might be SHP-2. The analysis of SHP-2 immunoprecipitates with the modified in-gel PTP assay confirms our hypothesis, showing that SHP-2 is transiently inactivated on integrin engagement (Fig. 4B). This inactivation starts at 10 min, is maximal at 45 min, and then returns to basal levels within 2 h of adhesion.

To confirm this finding, we analyzed the redox state of SHP-2 by using the redox-sensitive probe *N*-(biotinoyl)-*N*′-(iodoacetyl)-ethylenediamine (BIAM), which specifically labels molecules containing low-pKa cysteine residues. After BIAM labeling of the whole-cell lysate, SHP-2 was immunoprecipitated, and an HRP-avidin blot was performed to detect biotin-labeled, hence reduced, SHP-2. Within 10 min after cell adhesion, SHP-2 is oxidized and then by 2 h is reduced (Fig. 4C). Strikingly, the kinetics of SHP-2 redox regulation overlaps the oxidant burst during integrin-mediated signaling, suggesting that SHP-2 redox control might play a major role in focal adhesion formation and subsequent cytoskeleton remodeling after integrin stimulation. To explore the contribution of ROS produced in the early and late phase of adhesion, we analyzed the effect of the inhibitors rotenone and NDGA on the redox state of SHP-2. Our results show that SHP-2 oxidation within 10 min of adhesion is mediated by ROS produced by both mitochondria and 5-LOX, whereas in the late phase of adhesion, 5-LOX–mediated ROS production predominates in SHP2 oxidation (Fig. 4D).

Downstream effects of SHP2 oxidation during integrin-mediated adhesion

It has been proposed that increased production of ROS may contribute to enhanced tyrosine phosphorylation–dependent signaling (1, 2, 44) by transiently suppressing the enzymatic activity of members of the PTP family, thereby promoting a burst of protein tyrosine kinase activity (18, 19). Recent reports demonstrate that SHP-2 is involved in signaling inactivation because fibroblasts lacking a functional SHP-2 display reduced FAK dephosphorylation (52). Furthermore, cells overexpressing the dominant negative form of SHP-2 exhibit a larger number of focal adhesion contacts than did wild-type cells, suggesting that SHP-2 activity participates in the integrin-deactivation process (25). In addition to FAK, SHPS-1 has been reported to be among SHP-2 substrates. SHPS-1 is a transmembrane glycoprotein that becomes tyrosine phosphorylated in response to ECM contact (32, 46) and is required for Rho activation and cell motility in response to integrin stimulation (26). Hence, we analyzed the phosphorylation level of both FAK and SHPS-1 on integrin engagement (Fig. 5). Consistent with the kinetics of SHP-2 oxidation, during early adhesion, FAK tyrosine phosphorylation is sensitive to both NDGA and rotenone, thus suggesting that both mitochondria and 5-LOX–derived ROS are involved in this phase. Conversely, during late adhesion, FAK phosphorylation is sensitive mainly to NDGA and only to a lesser extent to rotenone, thus confirming that the main ROS pathway during late adhesion is 5-LOX rather than mitochondria (Fig. 5A). Antioxidant treatment on SHPS-1 phosphorylation on integrin-mediated stimulation gave similar results, although the contribution of mitochondrial ROS appears more relevant with respect to FAK phosphorylation (Fig. 5B). These findings suggest that transient SHP-2 inactivation by ROS may regulate cellular adhesion through an increase in tyrosine phosphorylation of specific signal-transduction proteins.

On the basis of these findings, we investigated the effect of intracellular ROS levels on cell adhesion and downstream targets, as p125FAK and SHPS-1 phosphorylation. Figure 6A shows the effect of the exogenous modulation of oxidants on integrin-mediated cell adhesion: the spreading of cells is increased during H_2O_2 treatment and decreased by NDGA administration, suggesting a key role of oxidants in the modulation of spreading. These results are in agreement with the already proposed role for H_2O_2 as second messenger during integrin-mediated cell adhesion affecting p125FAK phosphorylation through redox inhibition of p125FAK phosphatases (14). Moreover, H_2O_2 and NDGA treatments accordingly affect the phosphorylation level of p125FAK (Fig. 6B). To confirm that transient SHP-2 inactivation during cell adhesion is required for integrin-mediated cell spreading, we overexpressed both wild-type (wt) and the inactive dominant negative (dn) mutant of SHP-2 in ECM adhering cells. Regulation of SHP-2 enzymatic activity severely affects cell spreading, because cells overexpressing dnSHP-2, which mimics the effect of H_2O_2 treatment, display a marked increase in cell adhesion and spreading onto ECM ligands at 45 min when compared with wtSHP2-expressing ones (Fig. 6C). To support the key role of SHP-2 inactivation for correct cell spreading we analyzed the contribution of NDGA treatment to adhesion of cells overexpressing the inactive dnSHP2. We reported the ratio between NDGA-untreated and -treated samples in mock and dnSHP2 cells during cell adhesion. Figure 6D shows that in mock cells, NDGA cause a twofold increase in the ratio, whereas in dnSHP2 cells, the ratio is decreased to 1.4-fold, suggesting a strong, although incomplete, contribution of SHP2 redox inactivation to cell spreading. It is therefore likely that other redox-sensitive proteins involved in cytoskeleton rearrangement are targets of integrin-mediated ROS production. We recently reported that c-Src kinase and β-actin (17, 22) undergo redox regulation during cell adhesion, likely accounting for the SHP2-independent role of oxidants in the dynamic of cell spreading.

We then analyzed the phosphorylation level of SHP-2 substrates (p125FAK and SHPS-1) in cells overexpressing dn or wtSHP-2. In agreement with the observed phenotypic effect, during integrin-mediated cell adhesion, we detected an increased phosphorylation level of these substrates in cells overexpressing the dnSHP-2 mutant with respect to control cells. Conversely, the overexpression of wtSHP-2 leads to the opposite effect (Fig. 6E). Taken together, our results show that SHP-2 inactivation, either through oxidation or due to inactivating mutagenesis, similarly affects cell adhesion, leading to a faster and enhanced spreading. Hence, the inhibition of SHP-2 activity is instrumental for the correct cell adhesion and spreading.

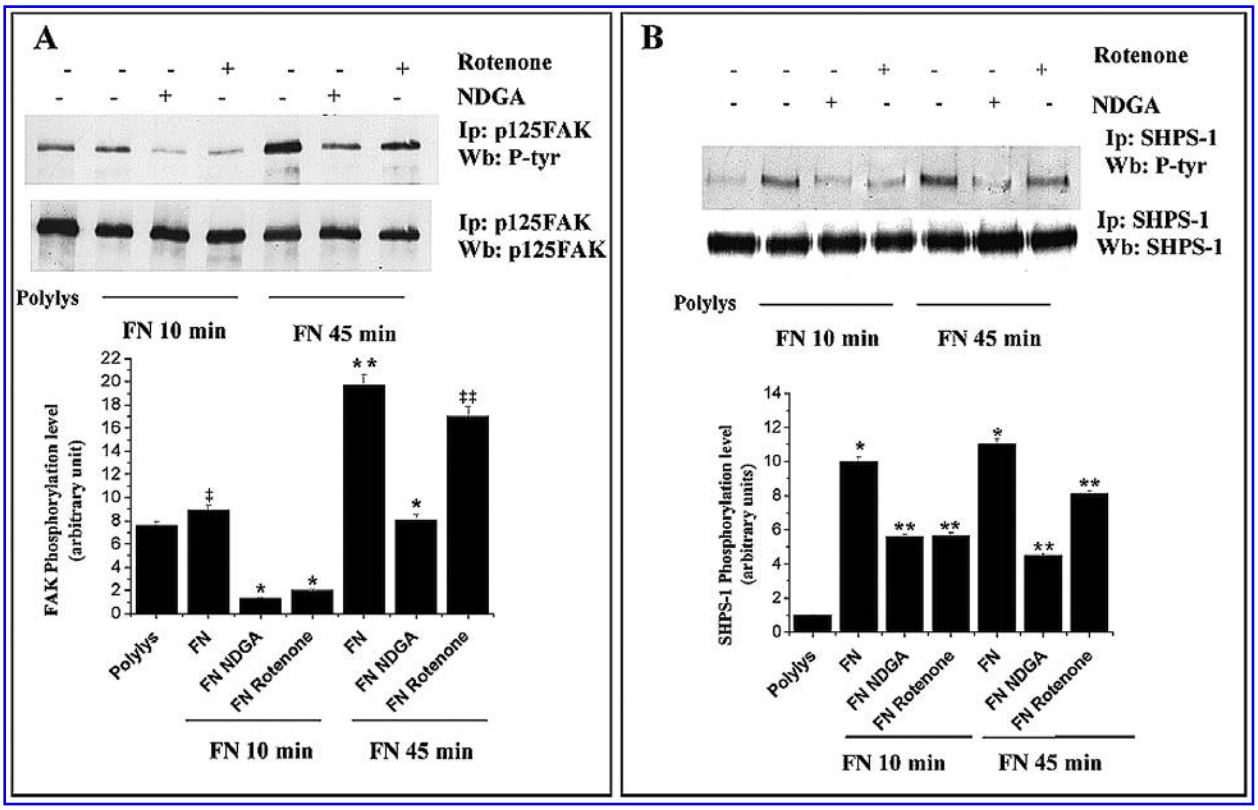

FIG. 5. SHP-2 oxidation affects FAK and SHPS-1 phosphorylation level. (**A**) NIH3T3 cells were serum starved for 24 h before detaching and maintaining in suspension with gentle agitation for 30 min at 37°C. Cells were then seeded onto polylysine- or fibronectin-coated dishes for the indicated times. The 10 μ*M* NDGA or 5 μ*M* rotenone was added for 20 min during the early and late phases of adhesion: for early adhesion, inhibitors were added 10 min before the end of suspension; for late adhesion, inhibitors were added 10 min after adhesion. Cells were then lysed in RIPA buffer. p125FAK was immunoprecipitated from total cell lysates, and an antiphosphotyrosine immunoblot was performed. The blot was then stripped and reprobed with anti p125FAK antibodies for normalization. A bar graph obtained from densitometry analysis of triplicate experiments normalized to loading controls is shown. ‡$p < 0.05$ vs. polylys; ‡‡$p < 0.05$ vs. FN at the same time; *$p < 0.001$ vs. FN at the same time; **$p < 0.001$ vs. polylys. (**B**) Cells were treated as in **A**, except that SHPS-1 was immunoprecipitated from total cell lysates, and an antiphosphotyrosine immunoblot was performed. The blot was then stripped and reprobed with anti SHPS-1. A bar graph obtained from densitometry analysis of triplicate experiments normalized to loading controls is shown. *$p < 0.001$ vs. polylys; **$p < 0.001$ vs. FN at the same time.

DISCUSSION

During cell adhesion, intracellular ROS production from both the mitochondrial respiratory chain and cytosolic 5-LOX acts as specific second messenger. The contribution of each pathway differs with respect to the kinetics of cell contact with the ECM and the organization of cytoskeleton: in the early phase of ECM contact, both ROS sources play a key role, whereas only 5-LOX–driven oxidants appear to guide the late phase of integrin-mediated cell spreading. Furthermore, we demonstrate that the increase in the intracellular ROS level causes a transient oxidation of SHP-2 that leads to an increase in tyrosine phosphorylation of its substrates FAK and SHPS-1, thus extending the propagation of the integrin signal. We believe that the novelty of our studies is joined to the dissection of the single contribution of 5-LOX and the mitochondrial respiratory chain during cell adhesion–mediated ROS production. Furthermore, we underscore the relevance of SHP-2 oxidation/inactivation for the correct execution of integrin-mediated cell spreading, thus including this phosphatase among other redox-sensitive proteins leading to the proper execution of cytoskeleton dynamics on ECM contact.

Recent reports demonstrated a key role for intracellular ROS during cell adhesion (14, 48), although disagreement exists about the metabolic pathway associated with oxidant production. Our aim was to clarify the different functions, if any, for mitochondrial- and cytosolic-derived ROS, which have been previously indicated as contributing to integrin-mediated cell adhesion. We demonstrate that mitochondrial and 5-LOX–derived ROS have different kinetics, with mitochondrial ROS confined to the beginning phase of cell spreading and 5-LOX–derived oxidants being extended all along the whole cell-spreading process and orchestrating the final cell shape. The physiologic significance of this distinct compartmentalization and kinetics is still unclear. It is possible that the different localization and timing of ROS production could be responsible for oxidation of distinct subsets of

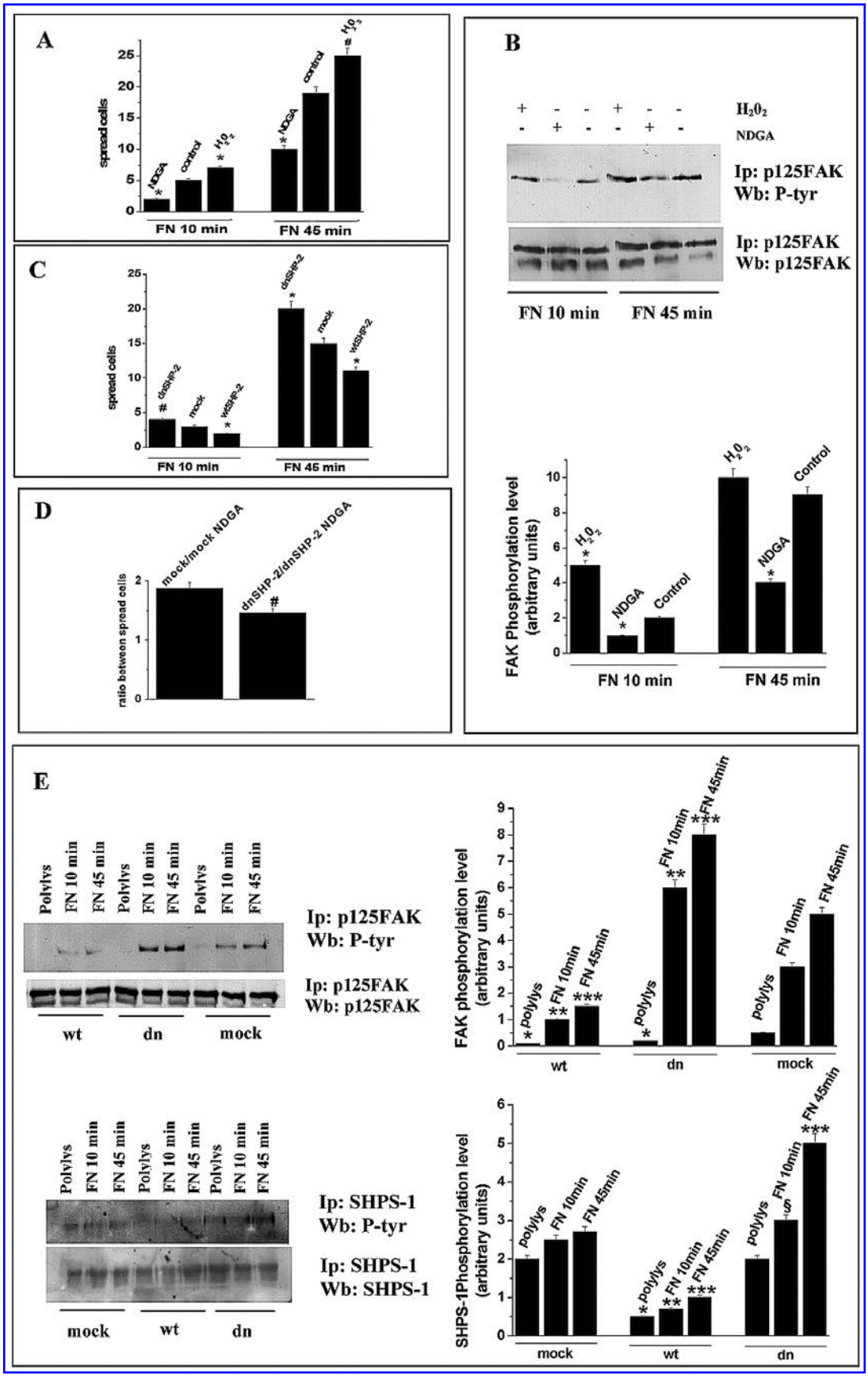
A
spread cells
NDGA
control
H2O2
FN 10 min
FN 45 min
B
H2O2
NDGA
Ip: p125FAK
Wb: P-tyr
Ip: p125FAK
Wb: p125FAK
FN 10 min
FN 45 min
FAK Phosphorylation level (arbitrary units)
Control
C
spread cells
dnSHP-2
mock
wtSHP-2
FN 10 min
FN 45 min
D
ratio between spread cells
mock/mock NDGA
dnSHP-2/dnSHP-2 NDGA
E
Polylys
FN 10 min
FN 45 min
Ip: p125FAK
Wb: P-tyr
Ip: p125FAK
Wb: p125FAK
wt
dn
mock
FAK phosphorylation level (arbitrary units)
Ip: SHPS-1
Wb: P-tyr
Ip: SHPS-1
Wb: SHPS-1
SHPS-1Phosphorylation level (arbitrary units)

redox-regulated molecular targets involved in the early or late phase of adhesion.

The differential effects of selective antioxidants on cell spreading and cytoskeleton organization enhances the concept that mitochondrial and cytoplasmic ROS play diverse roles, likely acting in promoting different events during cell adhesion. In particular, mitochondrial ROS could take part in the first cellular contact with ECM and focal adhesion formation, whereas cytoplasmic ROS could act during both phases, participating in the diffuse cytoskeleton remodeling and the formation of actin stress fibers. Adhesion is a dynamic process characterized by an initial phase promoted by interaction with ECM that leads to integrin clustering and development of small focal adhesions, followed by formation of more-stable and larger integrin-associated focal complexes, promoting cell spreading (7). The joint role that we demonstrate for mitochondrial and cytosolic ROS is in partial disagreement with the report of Werner and colleagues (48). They proposed mitochondria as the sole source of oxidants during integrin signal transduction, and in their cell model, rotenone alone is able to inhibit the increase in ROS content. This apparent discrepancy may be due to the different cellular models used in the adhesion studies. Although we reproduce the entire cell-adhesion process by seeding cells onto a physiologic ECM ligand coated to plastic dishes, Werner *et al.* (48) study only integrin-receptor ligation by soluble anti-α5 monoclonal antibodies. We propose that the model of Werner *et al.* may be helpful to investigate the early phase of cell adhesion (the engagement of integrin receptors), but cannot address the subsequent 5-LOX–dependent cell-adhesion steps, in particular those orchestrating the organization of cytoskeleton. Our findings indicate that oxidants exert their primary function during this late phase of cell adhesion. This conclusion is supported by the effect of antioxidant treatment of adherent cells, which causes a complete impairment of cell spreading and cytoskeleton rearrangement but allows cells to be firmly attached to the ECM substratum.

We recently reported that LMW-PTP and the tyrosine kinase c-Src are two redox-regulated proteins after integrin-mediated adhesion (14, 22). Herein we include in this group the SHP-2 phosphatase. We focused our attention on PTPs owing to the well-known role of this family of enzymes in cytoskeleton rearrangement (15) and for their sensitivity to oxidation of the active-site cysteine (10, 11, 31, 45). SHP-2 is a crucial component of RTK and integrin signaling, being recruited either to the receptors themselves or to receptor-associated docking proteins. A recent report demonstrates that SHP-2 is redox sensitive, because PDGF stimulation rapidly oxidizes and inactivates the enzyme (31). Here we report that SHP-2 is oxidized and hence inactivated during cell adhesion. This oxidation is transient and reversible, in keeping with the general idea of ROS generation as a tightly regulated event. In agreement with our demonstration of different sources of oxidants during early and late adhesion, we showed that both mitochondria and 5-LOX contribute to early SHP-2 oxidation, whereas the strongest oxidation of the phosphatase, solely due to 5-LOX activation, is reached at the time of cytoskeleton rearrangement.

The role of SHP-2 in integrin signaling has been controversial. Yu *et al*. (52) reported that fibroblasts lacking a functional SHP-2 were impaired in their ability to spread and migrate on fibronectin when compared with wild-type cells, suggesting a positive role of SHP-2 in promoting cell migration and spreading. In contrast, Schoenwaelder *et al*. (42) demonstrated that SHP-2 negatively regulates RhoA activity. RhoA is required for both formation and maintenance of stress fibers and focal adhesions. In agreement with these findings, they showed that inhibition of SHP-2 increases the basal level of active RhoA, thus increasing cell adhesion. Furthermore, Inagaki *et al*. (25) demonstrated that overexpression of a catalytically inactive mutant of SHP-2 increases the number of actin stress fibers and focal adhesion contacts. Moreover, Manes *et al*. (30) suggested a role for SHP-2 in the integrin-deactivation process, based on the observation that SHP-2 dominant negative overexpressing cells display a larger number of focal adhesions. More recently, Kwon *et al.* (28) demonstrated that Jurkat T cells overexpressing dominant negative SHP-2 show an increase in T cell–receptor–stimulated adhesion.

Our findings, in agreement with the Manes and Kwon reports, show SHP-2 as a negative regulator of integrin signaling. We propose that a key event for promoting cell adhesion

FIG. 6. Effect of ROS content and SHP-2 activity on cell spreading. (**A**) NIH3T3 cells were serum starved for 24 h before detaching and maintaining in suspension with gentle agitation for 30 min at 37°C. Cells were then seeded onto fibronectin-coated dishes for the indicated times with or without 1 μ*M* H_2O_2 or 10 μ*M* NDGA. Spread cells are counted in six randomly chosen fields for each sample, and the means ± SD values are shown in the bar graph. **p* < 0.001 vs. control at the same time; #*p* < 0.005 vs. control at the same time. (**B**) Total cell lysates were prepared from cells treated as in **A**, and p125FAK was immunoprecipitated. An antiphosphotyrosine immunoblot was performed. The blot was then stripped and reprobed with anti-p125FAK antibodies for normalization. A bar graph obtained from densitometry analysis of triplicate experiments normalized to loading controls is shown. **p* < 0.001 vs. control at the same time. (**C**) The dnSHP-2– and wtSHP-2–overexpressing NIH3T3 cells were serum starved for 24 h before detaching and maintaining in suspension with gentle agitation for 30 min at 37°C. Cells were then seeded onto fibronectin-coated dishes for the indicated times. Spread cells are counted in six fields randomly chosen for each sample, and the means ± SD values are shown in the bar graph. **p* < 0.001 vs. mock at the same time; #*p* < 0.005 vs. mock at the same time. (**D**) An adhesion experiment was performed. Mock and dnSHP-2–overexpressing NIH3T3 cells were treated with 10 μ*M* NDGA, and spread cells at 45 min are counted in six fields randomly chosen for each sample; the ratios between NDGA-untreated and -treated samples are shown as means ± SD in the bar graph. #*p* < 0.005 vs. mock. (**E**) Total cell lysates were prepared from cells treated as in **C**, and p125FAK and SHPS-1 were immunoprecipitated. Each sample was divided into two aliquots, and antiphosphotyrosine, anti-p125 FAK, or SHPS-1 immunoblots were performed. Two bar graphs obtained from densitometry analysis of triplicate experiments normalized to loading controls are shown. **p* < 0.001 vs. mock cells on polylys; ***p* < 0.001 vs. mock cells at 10 min on FN; ****p* < 0.001 vs. mock cells at 45 min on FN; §*p* ≤ 0.01 vs. mock cells at 10 min on FN.

and spreading is the transient oxidation and inactivation of SHP-2. Two lines of evidence support this idea. First, integrin-mediated oxidation of SHP-2 upregulates both p125FAK and SHPS-1 phosphorylation. These events contribute to the propagation of the integrin signal, as both p125FAK and SHPS-1 phosphorylation is involved in actin remodeling (34, 46). FAK is a nonreceptor tyrosine kinase involved in regulating cell spreading by modulating the turnover of focal adhesions (24, 39). In addition, integrin-induced phosphorylation of SHPS-1 mediates the recruitment and activation of SHP-2 (46). This SHP-2/SHPS-1 complex promotes a positive-feedback loop leading to Src and FAK activation during integrin signaling (46). Second, either redox-independent modulation of SHP2 activity or the modulation of intracellular ROS severely affects cell spreading. For example, integrin-mediated cell adhesion is decreased by either ROS removal or overexpression of active SHP-2, and this adhesion is increased by either exogenous H_2O_2 treatment or dnSHP-2 overexpression. Furthermore, we suggest that SHP-2 is the major redox-regulated phosphatase involved in the control of p125FAK and SHPS-1 phosphorylation during integrin engagement. In cells overexpressing LMW-PTP, p125FAK tyrosine phosphorylation is regulated by a transient oxidation of this phosphatase during ECM contact and cell spreading (14). The higher endogenous expression level of SHP-2, with respect to LMW-PTP in NIH3T3 fibroblasts, confers to SHP-2 a main role among these two phosphatases for p125FAK redox regulation during integrin-mediated cytoskeleton organization.

In conclusion, we report that both mitochondria and 5-LOX are engaged in ROS production during cell adhesion, with distinct kinetics and function during early and late adhesion. We also show that SHP-2 is one of the main PTPs targeted by ROS during cell adhesion and that its oxidation and inactivation are responsible for the organization of the cytoskeleton in response to ECM contact, exerting a positive feedback on the remodeling of the actin cytoskeleton and guaranteeing correct spreading.

ACKNOWLEDGMENTS

This work was supported by the Italian Association for Cancer Research (AIRC), by the Ministero della Università e Ricerca Scientifica e Tecnologica (MIUR-PRIN 2002), by Consorzio Interuniversitario Biotecnologie, and by Cassa di Risparmio di Firenze. We thank Anna Vestrini for technical support.

ABBREVIATIONS

BIAM, *N*-(biotinoyl)-*N′*-(iodoacetyl)-ethylenediamine; DCF-DA, 2′,7′-dichlorofluorescein diacetate; ECM, extracellular matrix; FAK, focal adhesion kinase; 5-LOX, 5-lipoxygenase; NBT, nitroblue tetrazolium; NDGA, nordihydroguaiaretic acid; PTP, protein-tyrosine phosphatase; ROS, reactive oxygen species; Rot, rotenone; RTK, receptor tyrosine kinase; SHP-2, Src homology-2 domain–containing phosphatase 2; SHPS-1, SHP- substrate.

REFERENCES

1. Bae YS, Kang SW, Seo MS, Baines IC, Tekle E, Chock PB, and Rhee SG. Epidermal growth factor (EGF)-induced generation of hydrogen peroxide: role in EGF receptor-mediated tyrosine phosphorylation. *J Biol Chem* 272: 217–221, 1997.
2. Bae YS, Sung JY, Kim OS, Kim YJ, Hur KC, Kazlauskas A, and Rhee SG. Platelet-derived growth factor-induced H(2)O(2) production requires the activation of phosphatidylinositol 3-kinase. *J Biol Chem* 275: 10527–10531, 2000.
3. Barcellos-Hoff MH and Dix TA. Redox-mediated activation of latent transforming growth factor-beta 1. *Mol Endocrinol* 10: 1077–1083, 1996.
4. Burridge K and Nelson A. An in-gel assay for protein tyrosine phosphatase activity: detection of widespread distribution in cells and tissues. *Anal Biochem* 232: 56–64, 1995.
5. Cadenas E and Davies KJ. Mitochondrial free radical generation, oxidative stress, and aging. *Free Radic Biol Med* 29: 222–230, 2000.
6. Cai J and Jones DP. Superoxide in apoptosis: mitochondrial generation triggered by cytochrome *c* loss. *J Biol Chem* 273: 11401–11404, 1998.
7. Carragher NO and Frame MC. Focal adhesion and actin dynamics: a place where kinases and proteases meet to promote invasion. *Trends Cell Biol* 14: 241–249, 2004.
8. Chandel NS, Maltepe E, Goldwasser E, Mathieu CE, Simon MC, and Schumacker PT. Mitochondrial reactive oxygen species trigger hypoxia-induced transcription. *Proc Natl Acad Sci U S A* 95: 11715–11720, 1998.
9. Chen Q, Olashaw N, and Wu J. Participation of reactive oxygen species in the lysophosphatidic acid-stimulated mitogen-activated protein kinase kinase activation pathway. *J Biol Chem* 270: 28499–28502, 1995.
10. Chiarugi P. PTPs versus PTKs: the redox side of the coin. *Free Radic Res* 39: 353–364, 2005.
11. Chiarugi P and Cirri P. Redox regulation of protein tyrosine phosphatases during receptor tyrosine kinase signal transduction. *Trends Biochem Sci* 28: 509–514, 2003.
12. Chiarugi P, Fiaschi T, Taddei ML, Talini D, Giannoni E, Raugei G, and Ramponi G. Two vicinal cysteines confer a peculiar redox regulation to low molecular weight protein tyrosine phosphatase in response to platelet-derived growth factor receptor stimulation. *J Biol Chem* 276: 33478–33487, 2001.
13. Chiarugi P and Giannoni E. Anchorage-dependent cell growth: tyrosine kinases and phosphatases meet redox regulation. *Antioxid Redox Signal* 7: 578–592, 2005.
14. Chiarugi P, Pani G, Giannoni E, Taddei L, Colavitti R, Raugei G, Symons M, Borrello S, Galeotti T, and Ramponi G. Reactive oxygen species as essential mediators of cell adhesion: the oxidative inhibition of a FAK tyrosine phosphatase is required for cell adhesion. *J Cell Biol* 161: 933–944, 2003.
15. Demali KA, Wennerberg K, and Burridge K. Integrin signaling to the actin cytoskeleton. *Curr Opin Cell Biol* 15: 572–582, 2003.
16. Djordjevic T, Pogrebniak A, BelAiba RS, Bonello S, Wotzlaw C, Acker H, Hess J, and Gorlach A. The expression of the NADPH oxidase subunit p22phox is regulated by a redox-sensitive pathway in endothelial cells. *Free Radic Biol Med* 38: 616–630, 2005.
17. Fiaschi T, Cozzi G, Raugei G, Formigli L, Ramponi G, and Chiarugi P. Redox regulation of beta-actin during integrin-mediated cell adhesion. *J Biol Chem* 281: 22983–22991, 2006.
18. Finkel T. Oxygen radicals and signaling. *Curr Opin Cell Biol* 10: 248–253, 1998.
19. Finkel T. Redox-dependent signal transduction. *FEBS Lett* 476: 52–54, 2000.
20. Finkel T. Oxidant signals and oxidative stress. *Curr Opin Cell Biol* 15: 247–254, 2003.
21. Flohe L and Otting F. Superoxide dismutase assays. *Methods Enzymol* 105: 93–104, 1984.
22. Giannoni E, Buricchi F, Raugei G, Ramponi G, and Chiarugi P. Intracellular reactive oxygen species activate Src tyrosine kinase during cell adhesion and anchorage-dependent cell growth. *Mol Cell Biol* 25: 6391–6403, 2005.

23. Griendling KK, Minieri CA, Ollerenshaw JD, and Alexander RW. Angiotensin II stimulates NADH and NADPH oxidase activity in cultured vascular smooth muscle cells. *Circ Res* 74: 1141–1148, 1994.
24. Ilic D, Furuta Y, Kanazawa S, Takeda N, Sobue K, Nakatsuji N, Nomura S, Fujimoto J, Okada M, and Yamamoto T. Reduced cell motility and enhanced focal adhesion contact formation in cells from FAK-deficient mice. *Nature* 377: 539–544, 1995.
25. Inagaki K, Noguchi T, Matozaki T, Horikawa T, Fukunaga K, Tsuda M, Ichihashi M, and Kasuga M. Roles for the protein tyrosine phosphatase SHP-2 in cytoskeletal organization, cell adhesion and cell migration revealed by overexpression of a dominant negative mutant. *Oncogene* 19: 75–84, 2000.
26. Inagaki K, Yamao T, Noguchi T, Matozaki T, Fukunaga K, Takada T, Hosooka T, Akira S, and Kasuga M. SHPS-1 regulates integrin-mediated cytoskeletal reorganization and cell motility. *EMBO J* 19: 6721–6731, 2000.
27. Knaus UG, Heyworth PG, Evans T, Curnutte JT, and Bokoch GM. Regulation of phagocyte oxygen radical production by the GTP-binding protein Rac 2. *Science* 254: 1512–1515, 1991.
28. Kwon J, Qu CK, Maeng JS, Falahati R, Lee C, and Williams MS. Receptor-stimulated oxidation of SHP-2 promotes T-cell adhesion through SLP-76-ADAP. *EMBO J* 24: 2331–2341, 2005.
29. Lee SR, Kwon KS, Kim SR, and Rhee SG. Reversible inactivation of protein-tyrosine phosphatase 1B in A431 cells stimulated with epidermal growth factor. *J Biol Chem* 273: 15366–15372, 1998.
30. Manes S, Mira E, Gomez-Mouton C, Zhao ZJ, Lacalle RA, and Martinez A. Concerted activity of tyrosine phosphatase SHP-2 and focal adhesion kinase in regulation of cell motility. *Mol Cell Biol* 19: 3125–3135, 1999.
31. Meng TC, Fukada T, and Tonks NK. Reversible oxidation and inactivation of protein tyrosine phosphatases in vivo. *Mol Cell Biol* 9: 387–399, 2002.
32. Oh ES, Gu H, Saxton TM, Timms JF, Hausdorff S, Frevert EU, Kahn BB, Pawson T, Neel BG, and Thomas SM. Regulation of early events in integrin signaling by protein tyrosine phosphatase SHP-2. *Mol Cell Biol* 19: 3205–3215, 1999.
33. Okuno H, Akahori A, Sato H, Xanthoudakis S, Curran T, and Iba H. Escape from redox regulation enhances the transforming activity of Fos. *Oncogene* 8: 695–701, 1993.
34. Owen JD, Ruest PJ, Fry DW, and Hanks SK. Induced focal adhesion kinase (FAK) expression in FAK-null cells enhances cell spreading and migration requiring both auto- and activation loop phosphorylation sites and inhibits adhesion-dependent tyrosine phosphorylation of Pyk2. *Mol Cell Biol* 19: 4806–4818, 1999.
35. Pani G, Colavitti R, Bedogni B, Anzevino R, Borrello S, and Galeotti T. A redox signaling mechanism for density-dependent inhibition of cell growth. *J Biol Chem* 275: 38891–38899, 2000.
36. Peppelenbosch MP, Tertoolen LG, Hage WJ, and de Laat SW. Epidermal growth factor-induced actin remodeling is regulated by 5-lipoxygenase and cyclooxygenase products. *Cell* 74: 565–575, 1993.
37. Rainwater R, Parks D, Anderson ME, Tegtmeyer P, and Mann K. Role of cysteine residues in regulation of p53 function. *Mol Cell Biol* 15: 3892–3903, 1995.
38. Reeves EP, Lu H, Jacobs HL, Messina CG, Bolsover S, Gabella G, Potma EO, Warley A, Roes J, and Segal AW. Killing activity of neutrophils is mediated through activation of proteases by K+ flux. *Nature* 416: 291–297, 2002.
39. Ren XD, Kiosses WB, Sieg DJ, Otey CA, Schlaepfer DD, and Schwartz MA. Focal adhesion kinase suppresses Rho activity to promote focal adhesion turnover. *J Cell Sci* 113: 3673–3678, 2000.
40. Rook GA, Steele J, Umar S, and Dockrell HM. A simple method for the solubilisation of reduced NBT, and its use as a colorimetric assay for activation of human macrophages by gamma-interferon. *J Immunol Methods* 82: 161–167, 1985.
41. Sanchez-Alcazar JA, Schneider E, Martinez MA, Carmona P, Hernandez-Munoz I, Siles E, De La TP, Ruiz-Cabello J, Garcia I, and Solis-Herruzo JA. Tumor necrosis factor-alpha increases the steady-state reduction of cytochrome b of the mitochondrial respiratory chain in metabolically inhibited L929 cells. *J Biol Chem* 275: 13353–13361, 2000.
42. Schoenwaelder SM, Petch LA, Williamson D, Shen R, Feng GS, and Burridge K. The protein tyrosine phosphatase Shp-2 regulates RhoA activity. *Curr Biol* 10: 1523–1526, 2000.
43. Schreck R, Rieber P, and Baeuerle PA. Reactive oxygen intermediates as apparently widely used messengers in the activation of the NF-kappa B transcription factor and HIV-1. *EMBO J* 10: 2247–2258, 1991.
44. Sundaresan M, Yu ZX, Ferrans VJ, Irani K, and Finkel T. Requirement for generation of H2O2 for platelet-derived growth factor signal transduction. *Science* 270: 296–299, 1995.
45. Tonks NK. Redox redux: revisiting PTPs and the control of cell signaling. *Cell* 121: 667–670, 2005.
46. Tsuda M, Matozaki T, Fukunaga K, Fujioka Y, Imamoto A, Noguchi T, Takada T, Yamao T, Takeda H, Ochi F, Yamamoto T, and Kasuga M. Integrin-mediated tyrosine phosphorylation of SHPS-1 and its association with SHP-2: roles of Fak and Src family kinases. *J Biol Chem* 273: 13223–13229, 1998.
47. Wang GL, Jiang BH, and Semenza GL. Effect of altered redox states on expression and DNA-binding activity of hypoxia-inducible factor 1. *Biochem Biophys Res Commun* 212: 550–556, 1995.
48. Werner E and Werb Z. Integrins engage mitochondrial function for signal transduction by a mechanism dependent on Rho GTPases. *J Cell Biol* 158: 357–368, 2002.
49. Woo CH, Eom YW, Yoo MH, You HJ, Han HJ, Song WK, Yoo YJ, Chun JS, and Kim JH. Tumor necrosis factor-alpha generates reactive oxygen species via a cytosolic phospholipase A2-linked cascade. *J Biol Chem* 275: 32357–32362, 2000.
50. Xu D, Rovira II, and Finkel T. Oxidants painting the cysteine chapel: redox regulation of PTPs. *Dev Cell* 2: 251–252, 2002.
51. Xu YC, Wu RF, Gu Y, Yang YS, Yang MC, Nwariaku FE, and Terada LS. Involvement of TRAF4 in oxidative activation of c-Jun N-terminal kinase. *J Biol Chem* 277: 28051–28057, 2002.
52. Yu DH, Qu CK, Henegariu O, Lu X, and Feng GS. Protein-tyrosine phosphatase Shp-2 regulates cell spreading, migration, and focal adhesion. *J Biol Chem* 273: 21125–21131, 1998.

Address reprint requests to:
Paola Chiarugi
University of Florence
Department of Chemical Sciences
Viale Morgagni 50
50134 Firenze, Italy

*E-mail:*paola.chiarugi@unifi.it

Date of first submission to ARS Central, July 20, 2006; date of final revised submission, October 5, 2006; date of acceptance, October 15, 2006.

This article has been cited by:

1. Lucia Laura Policastro , Irene Laura Ibañez , Cintia Notcovich , Hebe Alicia Duran , Osvaldo Luis Podhajcer . The Tumor Microenvironment: Characterization, Redox Considerations, and Novel Approaches for Reactive Oxygen Species-Targeted Gene Therapy. *Antioxidants & Redox Signaling*, ahead of print. [Abstract] [Full Text HTML] [Full Text PDF] [Full Text PDF with Links]
2. Lalchhandami Tochhawng, Deng Shuo, Shazib Pervaiz, Celestial T. Yap. 2012. Redox regulation of cancer cell migration and invasion. *Mitochondrion* . [CrossRef]
3. Elisa Ferro, Luca Goitre, Saverio Francesco Retta, Lorenza Trabalzini. 2012. The Interplay between ROS and Ras GTPases: Physiological and Pathological Implications. *Journal of Signal Transduction* **2012**, 1-9. [CrossRef]
4. Luca Goitre, Barbara Pergolizzi, Elisa Ferro, Lorenza Trabalzini, Saverio Francesco Retta. 2012. Molecular Crosstalk between Integrins and Cadherins: Do Reactive Oxygen Species Set the Talk?. *Journal of Signal Transduction* **2012**, 1-12. [CrossRef]
5. Tania Fiaschi, Giacomo Cozzi, Paola Chiarugi. 2012. Redox Regulation of Nonmuscle Myosin Heavy Chain during Integrin Engagement. *Journal of Signal Transduction* **2012**, 1-9. [CrossRef]
6. A. Ostman, J. Frijhoff, A. Sandin, F.-D. Bohmer. 2011. Regulation of protein tyrosine phosphatases by reversible oxidation. *Journal of Biochemistry* . [CrossRef]
7. P. A. Swanson, A. Kumar, S. Samarin, M. Vijay-Kumar, K. Kundu, N. Murthy, J. Hansen, A. Nusrat, A. S. Neish. 2011. Enteric commensal bacteria potentiate epithelial restitution via reactive oxygen species-mediated inactivation of focal adhesion kinase phosphatases. *Proceedings of the National Academy of Sciences* **108**:21, 8803-8808. [CrossRef]
8. Ann-Charlotte B. Svensson Holm, Torbjörn Bengtsson, Magnus Grenegård, Eva G. Lindström. 2011. Platelet membranes induce airway smooth muscle cell proliferation. *Platelets* **22**:1, 43-53. [CrossRef]
9. S. Menazza, B. Blaauw, T. Tiepolo, L. Toniolo, P. Braghetta, B. Spolaore, C. Reggiani, F. Di Lisa, P. Bonaldo, M. Canton. 2010. Oxidative stress by monoamine oxidases is causally involved in myofiber damage in muscular dystrophy. *Human Molecular Genetics* **19**:21, 4207-4215. [CrossRef]
10. Giovambattista Pani, Tommaso Galeotti, Paola Chiarugi. 2010. Metastasis: cancer cell's escape from oxidative stress. *Cancer and Metastasis Reviews* **29**:2, 351-378. [CrossRef]
11. Alejandra San Martín , Kathy K. Griendling . 2010. Redox Control of Vascular Smooth Muscle Migration. *Antioxidants & Redox Signaling* **12**:5, 625-640. [Abstract] [Full Text HTML] [Full Text PDF] [Full Text PDF with Links]
12. E Giannoni, T Fiaschi, G Ramponi, P Chiarugi. 2009. Redox regulation of anoikis resistance of metastatic prostate cancer cells: key role for Src and EGFR-mediated pro-survival signals. *Oncogene* **28**:20, 2074-2086. [CrossRef]
13. Luis Covarrubias, David Hernández-García, Denhí Schnabel, Enrique Salas-Vidal, Susana Castro-Obregón. 2008. Function of reactive oxygen species during animal development: Passive or active?. *Developmental Biology* **320**:1, 1-11. [CrossRef]
14. Hugo P. Monteiro , Roberto J. Arai , Luiz R. Travassos . 2008. Protein Tyrosine Phosphorylation and Protein Tyrosine Nitration in Redox Signaling. *Antioxidants & Redox Signaling* **10**:5, 843-890. [Abstract] [Full Text PDF] [Full Text PDF with Links]
15. E Giannoni, F Buricchi, G Grimaldi, M Parri, F Cialdai, M L Taddei, G Raugei, G Ramponi, P Chiarugi. 2008. Redox regulation of anoikis: reactive oxygen species as essential mediators of cell survival. *Cell Death and Differentiation* **15**:5, 867-878. [CrossRef]
16. Paola Chiarugi. 2008. From anchorage dependent proliferation to survival: Lessons from redox signalling. *IUBMB Life* **60**:5, 301-307. [CrossRef]